Experimental Methods in Chemical Engineering: Contact angles

Charles Bruel[a,1], Salomé Queffeulou[a], Theron Darlow[a], Nick Virgilio[a], Jason R. Tavares[a], Gregory S. Patience[a,2]

[a] *Department of Chemical Engineering, Polytechnique Montreal, C.P. 6079, Succ. CV Montreal, H3C 3A7, Quebec, Canada*

Abstract

The contact angle (CA) formed at equilibrium at the three-phase line of contact between a liquid, a solid and a gas may be expressed as a function of both the interfacial and surface tensions. Young first derived this thermodynamic relationship in 1805. In practice, multiple CA values are observed due to kinetic phenomena induced by evaporation, vapour adsorption, or swelling, and thermodynamic ones induced by roughness and surface chemical heterogeneities, even at molecular-scale. These non-ideal conditions result into an hysteresis, i.e. a difference between wetting and dewetting behaviours, and Young's equation rarely applies. Three measuring methods stand out for their applicability and reliability. In the *sessile drop* method, a syringe deposits a liquid drop on a flat surface and the contact angle is measured through optical means based on the drop shape. In the *Wilhelmy balance* method, the force required to immerse a solid plate in a bath of liquid is indirectly related to the contact angle. In the *Washburn capillary rise* method, the contact angle is derived from the rate at which a liquid rises by capillarity through a packed bed of powder. Employing probe liquids of various polarity, the free surface energy of the solid may be estimated. Over the last two years, ∼8600 published articles mentioned *contact angle* in their topic. Their main focus was either to develop the fundamental understanding of wetting science, or to assess the success of surface modification methods for the production of novel surfaces, composites, and membranes with enhanced wetting, adhesive, and filtration properties.

INTRODUCTION

Wetting science investigates the behaviour of liquids in contact with solid surfaces. It is at the cross-section of the fluid mechanics and surface sciences as it involves both the static shape taken by the liquid on the substrate at equilibrium, its dynamic behaviour when flowing, and -in between- its resistance

[1] charles.bruel@polymtl.ca
[2] gregory-s.patience@polymtl.ca

to flow.[1, 2] It deals with gas, liquid, and solid phases, and their interfaces. Thomas Young[3] is usually considered to be the father of the investigations in surface wetting, although some may trace it back to Galileo and beyond.[4]

Our first interaction with materials is through their surface, and our daily-life comfort relies on their wettability properties as they influence, for instance, our ability to protect or clean them. From an industrial perspective, wetting behaviour relates to liquid spreading behaviours, hydrophobicity and/or oleophobicity, and adhesive properties.[5, 6] Wetting affects common operations such as mixing, piping, draining, filtrating, condensing, or painting. Wetting tests are inexpensive and fast to implement (a typical test takes a few minutes). Although their interpretation may be tedious,[5, 4] they are one of the most surface sensitive methods with an analysis depth of 0.5-1 nm,[5] which corresponds to a monolayer.[7, 8, 9]

Here, we describe the basic elements behind the theory of wetting and contact angle sciences, the measurement methods to assess solid surfaces and powders, their uncertainties, and their main applications.

Theory of wetting and contact angle sciences

Surface tension and free surface energy

Wetting behaviour stems from differences in intermolecular cohesive interactions between the phases. A molecule located in the middle of a chemically pure medium is subjected to isotropic cohesive interactions: it is pulled with an equal intensity in every direction[10] (Figure 1.a). The same molecule, located at an interface, experiences an imbalance between the *inward* interactions with the other molecules of its kind and the *outward* interactions with the other phases. In most circumstances, *inward* interactions are stronger than *outward* ones and molecules will be more stable inside the medium than at its interface. Increasing the interfacial area requires energy to balance the loss in cohesive interactions experienced by the molecules brought to the interface. The *free surface energy* (measured in $\mathrm{mJ \cdot m^{-2}}$) is the energy required to increase the interfacial area by one unit of surface. Another approach is to measure the force that needs to be applied on the perimeter of a surface element to extend it. The *surface tension* (measured in $\mathrm{mN \cdot m^{-1}}$) is a work, it is the linear force that needs to be applied on the perimeter of a surface element to extend it by one unit of length. The first law of thermodynamics states that energy variations within a system equate the sum of the works and heat transfers applied to this system. The surface tension (a work) and the free surface energy are thus not rigorously equal from a thermodynamical point of view.[11] It is by neglecting any heat transfer that they are often considered as such and that a single symbol, γ (sometimes σ), is employed to represent them. A list of the main symbols used throughout the manuscript is provided in the Nomenclature section.

Young's equation

γ is a function of the interfacial composition and carries the subscripts: sl, lg, and sg, which refer to the solid-liquid, the liquid-gas, and the solid-gas interfaces.

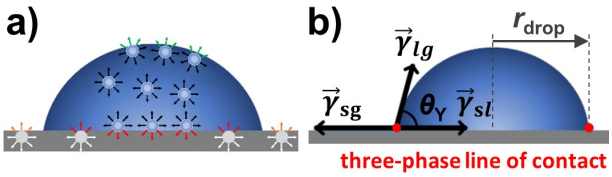

Figure 1: An imbalance in cohesive interactions between interfacial and core molecules is responsible for surface tension **(a)**. The droplet shape and the contact angle it forms at the solid surface derives from a force balance at the gas/liquid/solid three-phase line of contact, in red **(b)**. r_{drop} is the contact radius of the drop. Figure adapted from Yuan and Lee.[10]

The major contribution of Young[3] to the field of wetting was to write the force balance at the three-phase line of contact between an ideal solid substrate, the liquid and the gas phases (Equation 1, Figure 1.b). An ideal substrate is atomically flat, rigid, chemically homogeneous, and is unperturbed by the chemical interactions it may form with the probe liquid or its vapour.[4] The projection of the force balance in the solid surface plane, and perpendicularly to the three-phase line of contact, provides us with the modern form of the Young's equation (Equation 2), in which θ_{Y} is the contact angle formed by the liquid drop on the surface.[4] The force balance of Equation 1 does not include the strain field that forms in the solid below the three-phase contact line[12, 13, 4] and that balances the normal component of $\vec{\gamma}_{\text{lg}}$, $\gamma_{\text{lg}}\ sin\theta_{\text{Y}}$.[4] It is, however, of no consequences in the projected form of Equation 2. The latter also neglects the line tension Γ at the three-phase line of contact - this approximation is invalid in the case of droplets with micrometric or smaller dimensions.[14, 15] If r_{drop} is the contact radius of the drop (Figure 1.b), a contributing term in Γ/r_{drop} must be added to Young's equation: it is the Neumann-Boruvka's equation[16, 14] (Equation 3).

$$\vec{\gamma}_{\text{sg}} + \vec{\gamma}_{\text{sl}} + \vec{\gamma}_{\text{lg}} = \vec{0} \tag{1}$$

$$\gamma_{\text{sg}} = \gamma_{\text{sl}} + \gamma_{\text{lg}}\ cos\theta_{\text{Y}} \tag{2}$$

$$\gamma_{\text{sg}} = \gamma_{\text{sl}} + \gamma_{\text{lg}}\ cos\theta_{\text{Y}} + \frac{\Gamma}{r_{\text{drop}}} \tag{3}$$

The contact angle derived from Young's equation (Equation 2) is a static equilibrium contact angle. If θ_{Y} is below 90°, the liquid is said to wet the surface. If it is above 90°, the surface is said to be non-wetting for the liquid. If $\gamma_{\text{sg}} \geq \gamma_{\text{sl}} + \gamma_{\text{lg}}$, then $\theta_{\text{Y}} = 0$: the triple interface does not exist and the liquid totally wets the substrate.[4] Harkins and Feldman[17] formulated this condition more accurately in term of initial spreading coefficient for the formation of a duplex film upon spreading of a liquid. The initial spreading coefficient of a liquid b over a surface a, S_{ba}, is equal to the work of adhesion between b and a, W_{ba} minus the work of cohesion within b, W_b^c (Equation 4). If S_{ba} is positive, the liquid-surface adhesion trumps the liquid's cohesion: the liquid spreads over the surface.[17] γ_{a} and γ_{b} are the surface tensions of a and b in vacuum or in equilibrium with their own vapour.

$$\begin{aligned} S_{\mathrm{ba}} &= W_{\mathrm{ba}} - W_{\mathrm{b}}^{\mathrm{c}} \\ W_{\mathrm{ba}} &= \gamma_{\mathrm{b}} + \gamma_{\mathrm{a}} - \gamma_{\mathrm{ba}} \\ W_{\mathrm{b}}^{\mathrm{c}} &= 2\gamma_{\mathrm{b}} \end{aligned} \tag{4}$$

Harkins' theory on spreading,[17, 18] and its later developments,[19, 20, 21, 22] thus complete Young's equation (Equation 2). The latter even becomes a specific case of that wider theory for the spreading of a liquid over a surface in which $S_{\mathrm{ls}} = \gamma_{\mathrm{l}}(cos\theta_{\mathrm{Y}} - 1) < 0$ and in which the approximations $\gamma_{\mathrm{l}} \approx \gamma_{\mathrm{lg}}$, and $\gamma_{\mathrm{s}} \approx \gamma_{\mathrm{sg}}$ are made. The latter equates to neglecting the film pressure (also called spreading pressure), $\Pi_{\mathrm{s}} = \gamma_{\mathrm{s}} - \gamma_{\mathrm{sg}}$.[4, 11] This approximation is usually valid when $\theta_{\mathrm{Y}} > 10°$,[11] i.e. when $-S_{\mathrm{ls}} \gg 0$.

Contact angle hysteresis

The closest configuration to that described by Young's equation is that of a static liquid droplet deposited on a flat surface with a measured contact angle, θ. θ may differ from θ_{Y}, the Young contact angle.[23] At a moving three-phase line of contact, the angle formed by the liquid on the substrate is a dynamic contact angle. When the liquid advances from an already wet surface onto an unwet one, it is an advancing contact angle, θ_{a}. In the reverse situation, it is a receding contact angle, θ_{r}.[4] Advancing and receding contact angles are rate-dependent at high capillary number, Ca.[5] Ca is defined as the dimensionless ratio between the liquid viscosity, η_{l}, and its surface tension, γ_{lg}, times a velocity characteristic of the liquid's progression rate, V_{l}.[5] According to Strobel and Lyons,[5] a low capillary number ($Ca < 10^{-5}$) ensures that the contact angle measured at the moving three-phase line of contact is equal to that measured shortly after the liquid motion stops, i.e. that the dynamic CA measurement corresponds to a thermodynamically stable state.[23]

$$Ca = \frac{\eta_{\mathrm{l}} V_{\mathrm{l}}}{\gamma_{\mathrm{lg}}} \tag{5}$$

At low capillary numbers, θ_{a} and θ_{r} are respectively the highest and the lowest CA for which the droplet is in a meta-stable state over the surface: they correspond to local energy minima and θ_{r} is thus always less than or equal to θ_{a} ($\theta_{\mathrm{r}} \leq \theta_{\mathrm{a}}$).[23] In between, many other θ values, corresponding to other meta-stable states, may be measured ($\theta \in [\theta_{\mathrm{r}};\ \theta_{\mathrm{a}}]$). The most stable contact angle is measurable at the global energy minimum and can, under some circumstances, be related to Young's contact angle.[23] The difference between θ_{a} and θ_{r} is referred as the hysteresis, H ($= \theta_{\mathrm{a}} - \theta_{\mathrm{r}}$). It is null on ideal substrates[4, 5] where there is a single energy minimum and where the most stable contact angle is thus equal to θ_{Y}.[23] Experimentally, an hysteresis of 1-2° is achievable and considered as corresponding to an ideal configuration as it falls within the range of experimental error.[24, 4] In practice, very few real substrates may be considered as ideal[5] and an hysteresis in the range of 10° is common, while H may reach 50° or greater.[4] H increases with Ca.[25]

Description: experimental methods and instrumentation

Three methods to measure contact angles stand out for their applicability and reliability[10, 26]: the *sessile drop* (and its *tilted plate* variant), the *Wilhelmy balance*, and the *Washburn capillary rise* (WCR) methods (Table 1). The sessile drop method requires a flat substrate of a few mm^2, while a plate- or disk-like substrate –a few cm^2 large– is needed for the Wilhelmy balance method. The WCR method is best suitable with powders ($\sim$0.1 g to 10 g) of non-porous particles ($\sim$15 µm to 200 µm in diameter). Alternatively, powders (including those below 15 µm in diameter) may be cast or compressed into discs or plates for the sessile drop or the Wilhelmy plate methods.[26] Other techniques (non-discussed here) usually have even stricter requirements regarding solid geometry or operation conditions.[10, 26] They include the *captive bubble*, the *tilting plate* (not to be confused with the *tilted plate*), the *capillary tube*, the *individual fibre*, the *(capillary) dynamic contact angle*, the *environmental scanning electron microscopy (ESEM)*, and the *atomic force microscopy (AFM)* methods.[10, 26] The ESEM and AFM techniques are the cutting edge methods in wetting science as they are capable of analyzing μm^2 or nm^2 large surfaces with fL or zL liquid droplets, respectively. No method can accommodate every kind of sample geometries and dimensions, but in every situation, there is usually one that can.[10, 26]

Sessile drop method

The sessile drop method was the first CA goniometry method to be commercialized.[30, 10] A precision syringe, usually motorized, deposits a drop of probe liquid (of a few µL) on a flat substrate laying on a platform (Figure 1.b). A high resolution camera captures a cross section of the droplet. We estimate the static contact angle at the three-phase line of contact, θ, based on a fitting of the drop profile, usually with the Young-Laplace equation.[10]

The same setting can measure advancing and receding contact angles if the needle of the syringe is kept in contact with the liquid drop during the whole experiment.[30, 10] Upon slow ($Ca < 10^{-5}$) liquid dispensing, the drop grows (Figure 2.a). Inversely, a slow withdrawal of the liquid reduces the drop base diameter (Figure 2.b). We measure θ_a and θ_r at the moving three-phase line of contact, provided that the condition on the capillary number Ca is maintained. The sessile drop is a method that provides local wetting information (Table 1), screening of large samples thus requires to perform measurements on different areas of the substrate to obtain representative CA results. Kietzig[31] and Muller and Oehr[32] summarized the best practices for sessile drop measurements.

The *tilted plate* (or *inclined plate*) method is a variant of the sessile drop that can usually be performed with the same instrument.[10] A syringe deposits a drop of liquid on an horizontal substrate, which is then slowly inclined. The drop will gradually deform and lose its symmetry due to gravity: the maximum contact angle, θ_{max}, is found on the lower side of the drop and the minimum contact angle, θ_{min}, on the highest side (Figure 2.c). As the inclination of the plate increases, there is a point at which the drop will either slide or roll on the surface. The values of θ_{max} and θ_{min}, measured from a video footage

Table 1: Contact angle methods assuming kinetic hysteresis is negligible (see Strobel and Lyons[27] and Morra et al.[11] for methods to detect kinetic hysteresis). Controlled environmental rooms and anti-vibration systems increase measurements accuracy. The line *Complementary analysis* refers to characteristics of the solids required for reproducible contact angle measurements.

		Sessile drop (Figures. 1.b&2.a-b)	Tilted plate (Figure 2.c)	Wilhelmy balance (Figure 3)	Washburn capillary rise (Figure 4)
METHOD	Type	static dynamic	semi-static[a]	dynamic	dynamic
	Wetting	local	local	full (immersion)	full (capillarity)
	Test duration	∼min	∼min	∼min	∼h
SOLID	Geometry	flat surface	flat surface	disc/plate (no edge effect)	powder[b]
	Analyzed area	∼mm^2	∼mm^2	∼cm^2	∼m^2[b]
	Complementary analysis	roughness[c]	roughness[c]	roughness[c]	PSD[d] porosity[e]
LIQUID	Volume	∼µL	∼µL	∼mL	∼mL
	Progression	radial	-	axial	axial
	Contact angle requirements	error ↗ when $\theta_r < 20°$[10]	error ↗ when $\theta_r < 20°$[10]	-	$\theta_a < 90°$[26]
PARAMETERS	Known[f]	η_l, γ_{lg} drop volume or dispensing rate	η_l, γ_{lg} drop volume tilting angle	η_l, $\Delta\rho_{l-g}$, γ_{lg} solid geometry immersion depth	η_l, ρ_l, γ_{lg}
	Measured	photo/video t	video t	f t	ΔP t
	Calibrated	-	-	p[26]	r_{eff}[26]
	Calculated	Ca (Equation 5) θ or θ_a&θ_r[g]	θ_{min}&θ_{max}[g] sliding angle or rolling angle	Ca (Equation 5) V[h] θ_a&θ_r (Equation 6)	Ca (Equation 5) h (Equation 8) θ_a (Equation 7)

[a] Based on a video footage, measurement is taken just before the liquid begins to move[10].

[b] Average particle diameter between 15 and 200 µm[26]. The analyzed area depends on the particle specific surface area and mass (0.1 to 10 g)[26].

[c] Ratio between the surface area and the projected surface area[28].

[d] Particle size distribution[29].

[e] Particles shall not be porous in the WCR method[26].

[f] Environmental conditions (temperature, pressure, gas phase composition) must be reported.

[g] Image analysis and drop profile fitting[10].

[h] V is calculated from the solid geometry and the immersion depth.

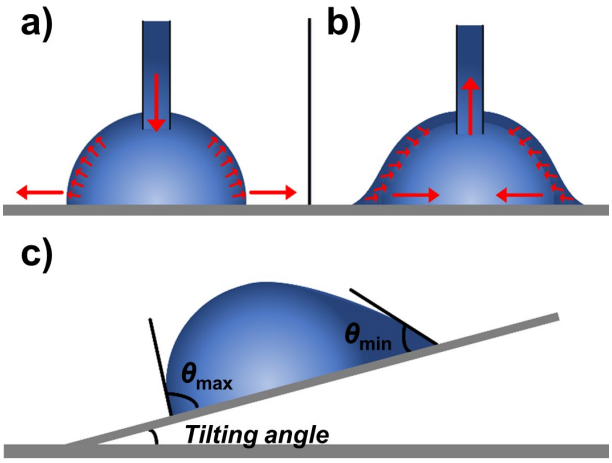

Figure 2: Optical goniometer dynamic contact angle methods. By injecting **(a)** or withdrawing **(b)** liquid within the drop, we measure the advancing or receding contact angles, respectively. In the tilted plate method **(c)**, the platform is slowly inclined until the droplet, having lost its symmetry, begins to move due to gravity. θ_{max} and θ_{min} are respectively the maximum and minimum contact angles formed by the asymmetric droplet on the surface. Figure adapted from Yuan and Lee.[10]

immediately before the drop begins to move are then assumed to be equal to θ_{a} and θ_{r}, respectively.[10] This method has to be used with great caution as significant deviations may exist between θ_{max} and θ_{a} on one side, and θ_{min} and θ_{r} on the other.[33, 34] Despite these flaws, the method remains industrially relevant as it enables for a measure of the sliding or rolling angle, i.e. of the tilting angle at which the drop begins to move, either by sliding or by rolling over the surface.[34, 25]

Wilhelmy balance method

Force tensiometers are the second most common goniometer type. Designed for the *Wilhelmy plate* or *Wilhelmy balance* method according to its first inventor,[35] a substrate of known shape (a plate, a disc or a beam[26]) and dimensions is slowly immersed in a fluid. When the suspended and initially non-immersed substrate contacts the liquid, a change in its apparent weight is detected. It is measured through the force variation, f, exerted by the substrate on the suspending system (Figure 3, steps 1&2). f is a combination of downward wetting forces applying at the interface, f_{w}, and of upward buoyancy, f_{b}. f_{w} is equal to the integral of the vertical component of $\vec{\gamma}_{\mathrm{lg}}$, $\gamma_{\mathrm{lg}}\ \cos\theta$, over the perimeter of the interface. θ is the contact angle formed by the liquid and the plate at the interface (Figure 3.b). If p is the total perimeter length of a homogeneous substrate, then $f_{\mathrm{w}} = \gamma_{\mathrm{lg}}\ p\ \cos\theta$. f_{b} equals the product of the total immersed volume V times $\Delta\rho_{\mathrm{l-g}}$, the difference in densities between the liquid and the gas phases, times g, the acceleration of gravity.

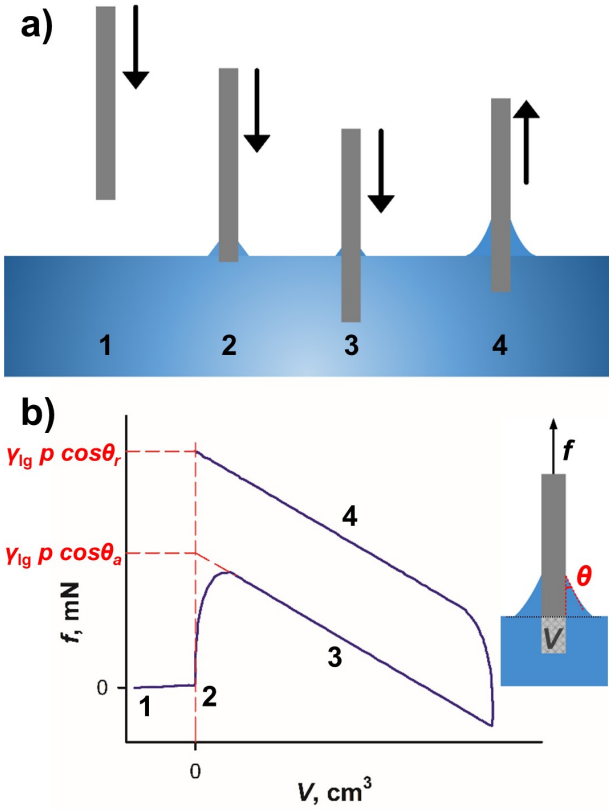

Figure 3: Wilhelmy balance method. During a cycle **(a)**, the initially unwet substrate (1) contacts the liquid (2), is immersed (3), and finally withdrawn (4). **(b)** The force variation experienced by the substrate during the process, f, is plotted as a function of the immersed volume, V. When the perimeter of the three-phase line of contact p is independent of V, f varies linearly with V in steps (3) and (4) (Equation 6). Extrapolating to $V = 0$ gives the advancing and the receding contact angle, respectively. Figure adapted from Yuan and Lee.[10]

$$f = f_{\mathrm{w}} - f_{\mathrm{b}} = \gamma_{\mathrm{lg}}\ p\ cos\theta - V\ \Delta\rho_{\mathrm{l-g}}\ g \tag{6}$$

Ideally, substrate preparation is such that p is independent of V (hence the preference for plate-like substrates), in which case f decreases linearly with V. An extrapolation of f in V=0 provides f_{w}, while the existence of an hysteresis translates into two different values for f_{w}, one linked to θ_{a} during the immersion (step 3 in Figure 6), and the other linked to θ_{r} when the substrate is pulled out of the liquid (step 4 in Figure 6). Average p can be approximated by performing a calibration with a zero contact angle ($\theta = 0$) probe liquid, usually a low surface tension liquid such as an alkane.[26]

Washburn capillary rise method

Both the *sessile drop* and the *Wilhelmy balance* methods require macro-sized flat surfaces. To estimate their liquid contact angle, powders can be cast or pressed into a film or a plate to fall into the previously described configurations.[26] Another possibility is to fill a capillary tube with powder and to analyze the progression of a rising fluid through the vertically-placed capillary, as one of its extremity is immersed into the probe liquid[26] (Figure 4.a). Assuming a Newtonian and incompressible fluid under a steady, laminar and fully developed flow with no slip conditions at the capillary walls, the velocity profile of the fluid is solved. Equation 7 is the integrated form of this velocity profile. It links linearly the square of h, the liquid height in the capillary, to t, the time of the experiment. The constant of proportionality is a function of the viscosity of the liquid, η_{l}, the effective radius, r_{eff}, γ_{lg} and cosθ. r_{eff} is the ideal cylindrical pore radius, assumed to be a function of the solid and of its packing only.[36, 26] Like p in the *Wilhelmy balance* method, it is a geometric parameter (expressed in meter) that can be calibrated with a low surface tension liquid, usually an alkane, for which $\theta_{\mathrm{a}} \approx 0$.[26] For $\theta_{\mathrm{a}} = 0$, Equation 7 indeed becomes a function of r_{eff} only. r_{eff} is then assumed to be constant and independent from the nature of the probe liquid.

$$h^2 = \frac{r_{\mathrm{eff}}\ \gamma_{\mathrm{lg}}\ cos\theta_{\mathrm{a}}}{2\eta_{\mathrm{l}}} t \tag{7}$$

Contact angles derived through Equation 7 are advancing contact angles and the WCR method do not provide any estimation for the hysteresis.[29] A typical experiment is divided into three phases (Figure 4.b): 1) an initial inertial regime during which the flow is established and h is roughly proportional to t; 2) the Washburn regime during which the flow is developed and where Equation 7 applies; and 3) a late viscous regime during which gravity predominates over the capillary forces.[26]

To increase precision, h variations are not measured through optical means but indirectly with a pressure transducer.[26] The latter assesses the rate at which the pressure drop, ΔP, decreases as the liquid rises. ΔP is the difference between the driving capillary pressure and the hydrostatic pressure ($\rho_{\mathrm{l}} g h$ = liquid density × acceleration of gravity × liquid height).[26] Assuming the capillary pressure to be a constant, the time dependency of h is then calculated from:

$$\frac{d\Delta P}{dt} = -\rho_{\mathrm{l}} g \frac{dh}{dt} \tag{8}$$

UNCERTAINTY

Limitations

Contact angle analysis are principally limited by the hypotheses regarding solid ideality (Equation 2). Deviations from ideal behaviour may be detected

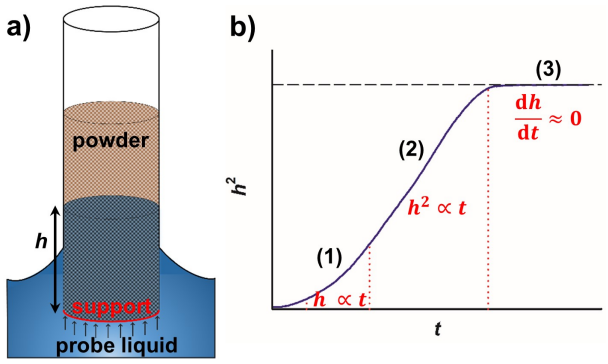

Figure 4: Washburn capillary rise (WCR) method setting **(a)**. The h over t dependency evolves during an experiment **(b)**: Phase (1) the inertial regime ($h \propto t$); phase (2) the Washburn regime (Equation 7: $h^2 \propto t$); phase (3) the late viscous regime (h reaches a plateau value). The advancing contact angle is derived from the Washburn regime.[26] Figure adapted from Alghunaim et al.[26].

through hysteresis, H. Literature considers two types of hysteresis: kinetic and thermodynamic.[4, 11, 5, 37]

Kinetic hysteresis arises from chemical interactions between the phases and a lack of stability of the different interfaces, which results in time-evolving contact angles.[38, 11, 5] Liquid evaporates at the gas/liquid interface: its influence may be especially acute in the sessile drop method where the volume of liquid is in the µL range, thus resulting in lower CA values.[4, 26] In other methods the volume of liquid and the interfacial area may be large enough to release a non-negligible amount of vapour in the atmosphere. It may then deposit at the gas-solid interface and pre-wet the substrate, which lessens θ_a measurements.[26] This feature, although detrimental to perform any measurement, may however be advantageously exploited for the calibration of the geometric parameters p and r_{eff} of Eqs. 6 and 7, respectively, by reducing the calibration liquid advancing contact angle.[26]

The most significant causes for kinetic hysteresis happen at the liquid/solid interface where any affinity of the substrate for the probe liquid may result into dissolution, penetration, swelling, or rapid reorientation of chemical functionalities at the substrate surface.[5] They all introduce systematic errors in θ_r as the liquid do not recede on the same substrate as the one on which it advanced. Dissolution, which includes the leaching of contaminant species, furthermore induces an evolution of the liquid surface tension over time. In advancing conditions, if the diffusion of the liquid at the surface of the substrate occurs faster than the rate of progression of the three-phase line of contact, then the measure of θ_a may be affected as well.

Thermodynamic hysteresis arises from heterogeneities at the surface of the substrate, be it of chemical or topographical (i.e. surface roughness) nature[39, 5] (Fig 5). A liquid advancing on a chemically inhomogeneous substrate tends to have its progression restrained by the lower free surface energy areas while a

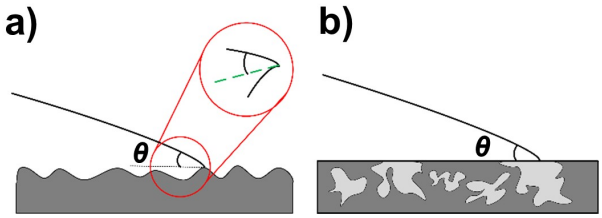

Figure 5: Surface roughness **(a)** and surface heterogeneity **(b)** are the two main causes of thermodynamical hysteresis.[39, 5] Figure adapted from Drelich et al.[39].

receding liquid will be held back by the higher free surface energy areas. It may translate into large hysteresis, almost 60° for water on various coal substrates as reported by Good et al.[40], for instance. Coal possesses lower and higher free surface energy carbonaceous components such as CH_2 and aromatic functions, respectively.[40] In practice, most substrates have surface heterogeneities that affect contact angle measurements.[5]

There is no consensus as to how flat a substrate has to be for roughness not to influence contact angle measurements.[41, 5] This influence is of two kinds as roughness affects both the amplitude of the hysteresis H and the contact angle values.[42, 43] In the homogeneous wetting regime, in which the liquid is considered to completely penetrate all of the surface cavities and pores,[23] contact angles increase with surface roughness on non-wetting surfaces (contact angle greater than 90°) and decrease on wetting surfaces (contact angle smaller than 90°).[42, 44] Young equilibrium contact angle θ_Y, as defined in Equation 2, thus cannot be measured directly for surfaces on which roughness is the primary cause for hysteresis. Instead, an apparent Young contact angle is obtained: the Wenzel contact angle, θ_W, which is equivalent to the most stable contact angle.[45, 23] θ_W relates to θ_Y through the Wenzel equation (Equation 9).[42] In this configuration, contact angle is indeed no longer a function of the free surface energy alone but also of its roughness, r_{surf}.[42, 41, 28]

$$cos\theta_W = r_{surf}\ cos\theta_Y \tag{9}$$

Strobel et al.[27] and Morra et al.[11] proposed strategies to study the time dependency of the hysteresis and isolate the thermodynamic component from the kinetics. The latter may be minimized by picking probe liquids that have a high boiling point and a low affinity for the substrate: any kinetic phenomenon must remain slow versus the duration of an experiment.[5, 4, 11] Thermodynamic hysteresis however provides information on surface roughness and chemical heterogeneity. Kwok and Neumann[41] categorized three different configurations for the thermodynamic hysteresis (provided that kinetic hysteresis is negligible): (1) ideal solids on which H=0 and where contact angles measured are equal to θ_W (= θ_Y, the surface is atomically flat); (2) flat chemically heterogeneous substrate on which both θ_a and θ_r are Young contact angles corresponding to the low and high free surface energy components of the surface; (3) rough

substrates for which, although H is characteristic of the roughness level, any measured CA value is meaningless in term of Young's equation (Equation 2). Indeed, while both the measured θ and θ_{W} ($\neq \theta_{\mathrm{Y}}$, the surface is rough) will be included between θ_{r} and θ_{a} ($\{\theta;\ \theta_{\mathrm{W}}\} \in [\theta_{\mathrm{r}};\ \theta_{\mathrm{a}}]^2$), there is no warranty that $\theta = \theta_{\mathrm{W}}$ and the uncertainty on the true value of θ_{W} is thus a growing function of H. Since θ_{W} corresponds to the most stable contact angle in the homogeneous wetting regime,[45, 23] it is however possible to relax the system to a repeatable CA measurement by providing enough vibrational energy to overcome the energy barriers existing between the different meta-stable states and the most stable state, i.e. between the various local energy minima and the global energy minimum.[46, 23] The method must be considered with caution as providing external energy may also lead to the transition from an homogeneous wetting regime to other wetting regimes (briefly described in the *APPLICATIONS* section).[15]

Detection limits

Chemical inhomogeneity

Hysteresis forms for large enough chemical surface heterogeneities. The definition of *large enough* is a function of the liquid surface tension and of the *quality of the heterogeneity*, meaning the difference between the Young contact angles formed by the probe liquid with the different surface chemistries, $\Delta\theta_{\mathrm{Y}}$. It decreases if γ_{lg} and $\Delta\theta_{\mathrm{Y}}$ increase.[47, 48] It ranges from 6-12 nm (γ_{lg}=70 mN $\cdot$ m^{-1} $\Delta\theta_{\mathrm{Y}}$=70°)[48] to ∼0.1 µm ($\gamma_{\mathrm{lg}}$=50 mN $\cdot$ m^{-1} $\Delta\theta_{\mathrm{Y}}$=10°).[47]

Surface roughness

Molecular scale variations in terms of surface roughness or substrate rigidity may explain the formation of hysteresis as high as 15°[49] and increase apparent equilibrium contact angles by as much as 10° to 20°.[50] There is thus probably no common substrate flat enough to totally avoid surface roughness effects.[5] In some cases, topographically induced hysteresis is however negligible, either in front of the measurement error, or in front of other forms of hysteresis.[40] Any serious study on contact angle should thus be supported by other topographical analysis methods like atomic force microscopy.[50, 28]

Sources of error

Strobel and Lyons[5] notes that a common error is to forget to check the solubility of surface components with the probe liquid and its influence on the liquid surface tension. It includes the influence of potential surface contaminants: thorough sample cleaning and handling protocols improve the repeatability of CA measurements.[51] Greater precision may also be achieved with a controlled atmosphere (composition, temperature).[4] A dry environment is especially relevant for hygroscopic probe liquids such as dimethyl sulfoxide.[4] These recommendations are part of the process to minimize kinetic hysteresis. Vibrations should also be avoided as they lower advancing contact angle measurements (up to several degrees).[52, 23] If we assume that sources of kinetic hysteresis have

been detected[27, 11] and addressed, that levels of surface roughness have been checked to be comparable from sample to sample, that dynamic contact angles are taken for $Ca < 10^{-5}$, and that the initial purity level of the probe liquids have been checked, then remaining sources of errors are mostly technique dependent. Owing to the easy acquisition of contact angle data, statistical analysis in term of standard deviations and confidence intervals are recommended.[5]

Working with an optical goniometer and drop-based methods, errors arise from the lack of axisymetry of the drop[2] and from the fitting of an equation –Young-Laplace or another[10]– on the drop shape[30]. Observed from the top, the droplet must be axisymetric for any CA derived from a side-view analysis to be meaningful.[2] On this side-view, baseline detection and luminosity induced mistakes are difficult to detect and correct, introducing an *operator error*. Automated fitting does not suppress it completely as it shifts the issue from the operator to the quality of the image and its contrast. In advancing and receding contact angle measurements, the presence of the needle in the drop (Figure 2) deforms its shape. Choosing a needle diameter small versus the drop width reduces this error.[30] While measuring receding contact angle, the operator must check that the front of the liquid recedes, especially when large H are reported and that a significant volume of liquid has to be withdrawn for the liquid to recede.[53] Drop-based methods are also subject to the *drop-size effect*: contact angle measurements vary slightly with the size of the drops.[11] The magnitude of the *drop-size effect* is however small in front of other incertitude sources,[11] unless working with micrometrically scaled drops, in which case the line tension, Γ, has to be considered (Equation 3).[14, 15] Overall, a reproducibility of $\sim \pm 2°$ on contact angle values is usually achievable through optical goniometers.[10] This uncertainty increases for low contact angle measurements ($< \sim 20°$): as the drop profile flattens, it becomes tedious to detect its baseline.[10]

The Wilhelmy plate method probes larger surface areas making it less sensitive to small surface defects and the three-phase line of contact is advancing in a single direction.[5, 10] It however requires increased volume of probe liquid ($\sim$mL) and larger substrate surfaces ($\sim$cm^2, Table 1). If the method is error-free in term of operator to operator variability,[54, 5] the calibration step, required to determine the value of the geometrical parameter p (Equation 6), however introduces a systematic error.[32, 55, 26] On the contrary, the sessile drop method enables for local wettability analysis while the three-phase line of contact has a radial progression.[55, 5, 10] Selection of the experimental method can help mitigating kinetic hysteresis effects: the contamination of the probe liquid phase, by dissolution of surface components, can for instance be reduced by increasing the ratio of probe liquid volume over mass of leached surface species.[51]. Due to its larger probe liquid volume (Table 1), the Wilhelmy balance method was hence found to be more pertinent than sessile drop for the analysis of surfaces releasing large amount of contaminants, while tuning the geometry of the probe liquid reservoir may further slow the contamination.[56, 51]

Alghunaim et al.[26] reviewed the methods to minimize measurement and sample preparation-linked errors in the WCR method. Inadequate particle size results in significant deviations: an average diameter above 200 µm causes pres-

sure drop variations (Equation 8) that are below the sensitivity level of common pressure transducers, while an average diameter below 15 µm translates into too small effective radii, r_{eff} (Equation 7).[26] As in the Wilhelmy plate method, the calibration of r_{eff} introduces a systematic error (see section *Limitations*). The powder shall not have any internal pores and the packing has to be as identical as possible between the different capillaries. Furthermore, the probe liquid must be such that $\theta_{\text{a}} < 90°$ for the method to work.[26]

APPLICATIONS

The four main categories of applications for contact angle measurement methods are:

1. investigations of wetting behaviours (hydrophobicity, oleophobicity, etc...);
2. surface property analysis (determination of hysteresis causes);
3. estimation of the substrate's free surface energy, γ_{sg}, and adhesive properties;
4. derived applications: emulsions, solid dewetting, catalyst ageing.

Investigation of specific wetting behaviour is the most obvious application with the characterization of water-repellent or oleophilic properties for a solid or a coating, for instance.[44, 57] For these applications, contact angle measurements is the most suitable technique to assess the success of a surface modification as it may often be performed with the liquid of interest. Increasing the substrate free surface energy wets the surface completely.[44, 4] Repelling liquid however requires to decrease the substrate free surface energy.[58] Contact angle hysteresis causes stickiness of the liquid over the surface[19] and sliding/rolling angles are especially relevant for the characterization of repelling properties as they provide a direct measurement of the force required to put droplets into motion and thus to remove them from the surface, with applications for the production of self-cleaning materials for instance.[25] Roughness is a two-level parameter: it increases the apparent contact angles on hydrophobic surfaces in the homogeneous wetting regime[42] (Figure 6.a). But in the case of highly structured micro- and nanoroughness, the liquid might not penetrate and wet all of the surface cavities thus leaving air pockets trapped at the substrate surface[57, 44] – it is the heterogeneous wetting regime (Figure 6.b). Liquid forms a 180° contact angle with these air pockets[44]: the apparent free surface energy of the solid decreases and the apparent liquid contact angle increases. As modeled by Cassie and Baxter,[43] surface texturing can produce super-repelling surfaces (contact angles above 150°). Using this principle, fine tuning of the wetting properties is achievable by replacing air by a given liquid.[59, 60] Those configurations may be described by the impregnated Cassie model.[61, 62, 63, 15] Situations that can be totally described by the traditional Cassie and Baxter model, or by the Wenzel model, are however relatively rare.[15] A model for mixed wetting was

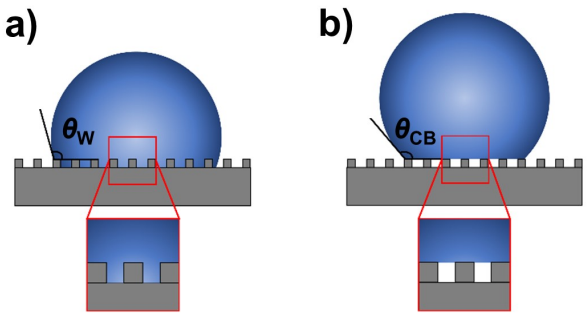

Figure 6: Homogeneous **(a)** and heterogeneous **(b)** wetting regimes on rough substrates. They are respectively governed by the Wenzel[42] (W) and the Cassie-Baxter[43] (CB) models. When the cavities at the solid substrate are filled by gases, the contact angle formed by a liquid droplet on a same substrate will be higher in the heterogeneous wetting regime than in the homogeneous one: $\theta_{CB} > \theta_{W}$.[57, 44, 58] Figure adapted from Yan et al.[58].

thus proposed,[64, 57] in which the homogeneous regime applies on a fraction of the surface while the heterogeneous regime is considered for the remaining areas where the liquid is in contact with air pockets. Various factors, recently reviewed by Bormashenko,[15] can trigger the transition from a wetting regime to another on rough surfaces. Understanding of the causes and mechanisms of these wetting transitions is critical to produce surfaces with stable and durable wetting properties.[15]

Due to its fine molecular-level detection limits in term of roughness and surface composition, the surface properties of a substrate may be explored by measuring the contact angle hysteresis and attributing its causes.[5] CA measurements are not self-sufficient and complementary techniques such as atomic force microscopy or surface elemental analysis are required for the interpretation.[4, 5, 50]

By performing the previous hysteresis analysis for several probe liquids, the Young contact angles between the substrate and the liquid set may be estimated. Equation 2 may then be reversed to estimate the free surface energy of the solid based on that of the probe liquids.[65, 4, 41] Indeed, γ_{sl} is a mathematical function of γ_{sg} and γ_{lg}[41]: $\gamma_{sl} = f(\gamma_{sg}, \gamma_{lg})$. If we define $F(\gamma_{sg}, \gamma_{lg}) = \gamma_{sg}$ - $f(\gamma_{sg}, \gamma_{lg})$, then Equation 2 can be rewritten as:

$$\gamma_{lg}\ cos\theta_{Y} = F(\gamma_{sg}, \gamma_{lg}) \tag{10}$$

Several models have been proposed for F,[41, 32] the most popular being the one-parameter model of Zisman,[66, 11] the two-parameter model from Owens-Wendt-Rabel-Kaelble (OWRK), in which γ is divided in term of dispersive and polar components,[67] and the three-parameter acid-base model from Van Oss-Chaudhury-Good, in which the polar component of surface tension is itself divided into an acidic and basic contributions.[65, 4] Due to the difficulty to make sure that measured CA are Young contact angles, surface energies yielded by the method are often an approximation. The wording of *estimated free surface energy* has been recommended.[5] Estimated free surface energy parameters de-

Table 2: Typical step by step procedure for CA data acquisition and analysis.

	Step	Description
PRIOR-	**1**	Identify the best method based on the solid size and geometry (Table 1).
	2	Check the reproducibility of sample preparation (roughness for surfaces, particle size distribution for powders, solid packing for the WCR method, etc...)[26].
ACQUISITION	**3**	Select a suitable probe liquid to minimize kinetic hysteresis effects.[27, 11]
	4	Perform a calibration if needed (p or r_{eff} in the Wilhelmy balance and WCR methods, respectively).[26]
	5	Contact angle measurements (check the value of the Ca number[5]).
	6	Derive θ_{a} and θ_{r}, calculate their uncertainties.
	7	Estimate H.
POST-	**8**	Perform complementary analysis to attribute hysteresis causes.[5, 11, 4] If kinetic phenomena are the principle source of hysteresis, return to step **(3)** to select a more suitable probe liquid or to step **(1)** if there are reasons to believe that selecting another method can help mitigating kinetic phenomena. If thermodynamic features (roughness and chemical heterogeneities) are responsible for the hysteresis, determine in which configuration we are (1, 2 or 3 – see section *Limitations*)[41].
	9	If the Young contact angles, θ_{Y}, of the solid with several probe liquids are known, apply a model (Equation 10) to estimate the free surface energy of the solid.[65, 4, 41]

termined through contact angle measurements may then be employed to investigate adhesive properties.[4, 68] If we write a typical step by step procedure for CA data acquisition (Table 2), the number of steps required to draw conclusions increases with the complexity of the information seek from CA measurements. We can stop at ∼step 7 for type 1, at ∼step 8 for type 2 and at ∼step 9 for type 3 applications.

All the thermodynamic concepts derived here at the air/liquid/solid three-phase line of contact are also valid at the liquid/liquid/solid and liquid/liquid/liquid three-phase contact lines with, for instance, obvious applications in multiphase emulsions[69, 70, 20] and polymer blend morphology.[21, 22, 71, 72] At the air/solid/solid three-phase contact line, the thermodynamic equilibrium state is simply prevented by kinetic considerations.[73, 74] Upon heating, and even far below their melting point, solid thin films however recedes according to a dewetting process.[73, 74] This phenomenon is surface tension-driven and has applications in catalyst preparation.[75, 76] It also explains catalyst ageing: nanoparticles coalesce upon heating through surface diffusion of their constituents to minimize their surface tensions in an Oswald ripening process, thus reducing the overall surface area and the catalyst performance.[77, 78]

Relevant fields for CA measurements

We performed a literature survey of the articles published between 2016 and 2017 through the Web of Science™ Core Collection search engine.[79] ∼8600

entries mentioned *contact angle* in their topic. The three top categories were *Chemistry, Physical* (791 entries), *Materials Science, Multidisciplinary* (774), and *Engineering, Chemical* (464). 337 articles were published in *RSC Advances*, 317 in *Applied Surface Science*, and 224 in *Langmuir*. It represents respectively 1.7, 6.3, and 7.1 % of the articles published in these journals over the 2016-2017 time frame. Using the bibliometric network option of VOSviewer,[80, 81] the 102 most-common keywords were plotted in a graph (Figure 7) in which the font and the dot sizes are proportional to the keyword occurrence (from ∼95 to ∼1400). The number of links was limited in order to highlight the main connections.

VOSviewer identified 4 distinct clusters among the ∼8600 articles, each of them being represented by a color (blue and purple clusters being two subdivisions of a same cluster). *wettability* and *contact angle* science are the main subjects in the red cluster. It includes keywords such as *contact angle hysteresis*, *surface tension*, *surface energy*, *roughness*, *dynamics*, *model*, or *mechanism*. The blue+purple cluster is more oriented toward the production of surfaces with specific wetting properties with keywords such as *fabrication*, *design*, and *deposition* matching those of *coatings* and *surfaces* with properties like *superhydrophobicity*, *resistance*, and *transparent*. Keywords highlighted in purple are those that, although being mostly in relation with blue keywords, are of interest for other clusters, as evidenced by the citation links. Polymer chemistry and composites make up the green cluster. These studies often focus on biologically relevant systems, membranes, biomolecule-substrate interactions, and adhesive properties. The last cluster, in yellow, is related to nanoparticles, and their filtration (*removal*, *separation*).

Since 2016, the *Can. J. Chem. Eng.* published seventeen articles related to contact angles. In five of these papers,[82, 83, 84, 85, 86] CA is only an inlet parameter in a model or a numerical simulation. The twelve remaining involve experimental measurements, all of which performed with an optical goniometer[87, 88, 89, 90, 91, 92, 93, 94, 95] or derived instruments.[96, 97, 98] The latter enable analysis at a liquid/liquid/solid[97, 98] or a liquid/gas/solid[96] interface instead of a gas/liquid/solid one (Figure 1). Works performed with an optical goniometer mainly employed the static sessile drop method[87, 88, 89, 91, 92, 93, 94] with only two employing dynamic methods.[90, 95] Three studies included qualitative surface analysis through scanning electron microscopy images to estimate the substrate roughness[87, 90, 95]: Ahmmed et al.[90] published the only manuscript in which both advancing and receding contact angles are reported and in which an estimation of the hysteresis is provided.

Studies containing experimental work on contact angles were mostly interested in investigating the wettability of powders: nanoparticles[87, 88, 92, 93, 96, 98] and microparticles.[89, 91, 95, 97] Other surfaces of interest included polymeric films,[90] rocks,[98] and glass.[94] Powders were usually either cast or pressed into films and pellets to perform CA measurement. In one case, it was deposited on larger macroscopic surfaces[98]; in the two other, nanoparticles were left in suspension to act as modifiers of a liquid, water[96] or bitumen,[97] physical properties (viscosity, thermal conductivity, surface tensions). Probe liquids employed include water,[87, 88, 89, 90, 91, 92, 93, 96, 98] salted water,[97] toluene,[88, 92]

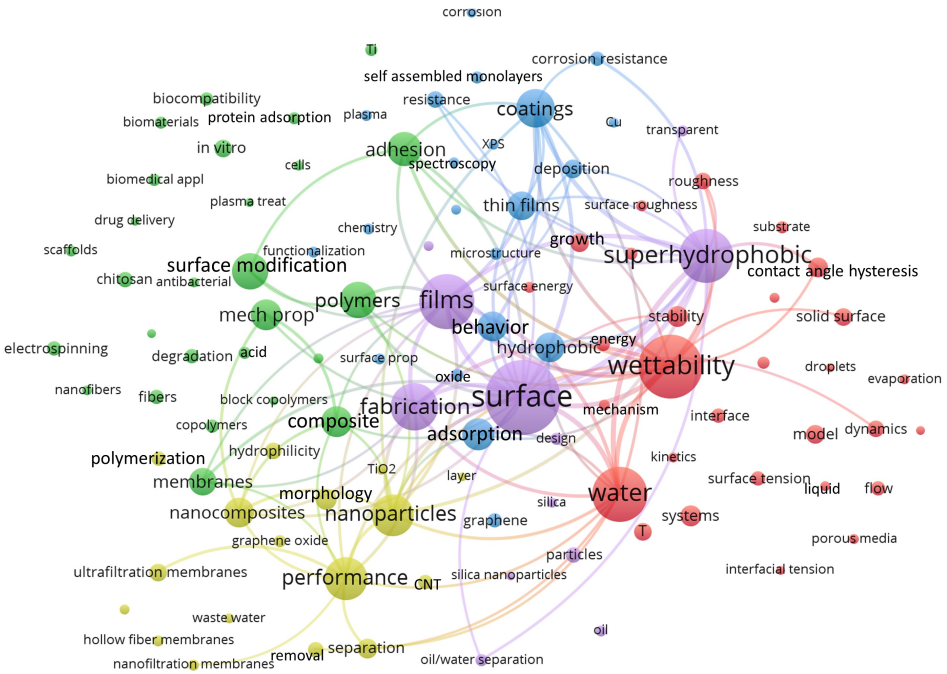

Figure 7: *Contact angle* bibliometric map:[80, 81] between 2016 and 2017, ∼8600 articles referenced by Web of Science have *contact angle* in the topic search field. The VOSviewer graph shows the top 102 keywords: font size is proportional to the keyword occurrence (from ∼95 to ∼1400); the lines represent citation links.

denatured ethanol,[92] n-dodecane,[92] bitumen,[97] and various oils.[94, 95, 98]

Contact angle measurements were performed in order to probe the wetting behaviour (usually hydrophobicity or oleophilicity) and assess the success of a modification method[87, 88, 89, 90, 91, 92, 93, 94, 98] (application (1), red cluster in the Figure 7). In two circumstances the hysteresis was investigated (application (2)), either in term of kinetic hysteresis (penetration of the liquid in a porous substrate)[95] or in term of surface anisotropy,[90] while in another the free surface energy of the solid was estimated through the OWRK model[92] (application (3)). Vafaei[96] performed a theoretical work by deriving two analytical expressions to refine Young's equation (Equation 2) and predict contact angles formed by gas bubbles and droplets growing underwater (blue cluster, Figure 7).

Out of the 17 articles identified in the *Can. J. Chem. Eng.*, only 6 mentioned *contact angle* in their topic (two numerical[82, 86] and four experimental[91, 92, 93, 96] works). Amongst the 11 remaining studies, contact angle measurements were deemed to be too insignificant to be mentioned in the title, the abstract, or the keywords. Such a pattern, if extendable to the broader literature, would mean that the database on which Figure 7 is built is incomplete, with a total number

of articles published containing contact angle related results between 2016 and 2017 closer to ∼20-25 thousands, instead of ∼8600.

CONCLUSIONS

Contact angle measurements is the science of probing surfaces with liquid molecules. The three most common methods to acquire CA are the sessile drop, the Wilhemly balance, and the Washburn capillary rise. Of particular industrial interest due to the wide range of applications requiring wet steps, contact angle measurements may provide molecular scale information in term of surface chemical composition and roughness. Those are indeed responsible for a thermodynamic hysteresis between the advancing and receding angle values. Acquiring exploitable thermodynamic data however requires avoiding kinetic phenomenons such as evaporation, swelling, or dissolution. Performed with several probe liquids of different polarity, it enables for an estimation of the solid free surface energy. Between 2016 and 2017, ∼8600 published articles mentioned *contact angle* in their title, their abstract, or their keywords. Besides fundamental works on wetting science, the hottest topics for contact angle measurements were the production and the characterization of surfaces and membranes with specific wetting, adhesive, or filtration properties. Future of the field lies in the refinement of the equations and models to better account for non-ideal behaviours and in the development of protocols minimizing hysteresis causes or enabling measurements at the nanoscale such as the atomic force microscopy and the environmental scanning electron microscopy methods.[10]

NOMENCLATURE

γ	Surface tension or free surface energy (approximated as equals).
γ_s, γ_l	γ measured at the interface of the solid (s), or of the liquid (l), with vacuum or at equilibrium with its own vapour.
γ_sg, γ_sl, γ_lg	γ measured at the solid/gas (sg), solid/liquid (sl), or liquid/gas (lg) interfaces, respectively.
Γ	Line tension at the three-phase line of contact.
Π_s	Film pressure (also called spreading pressure).
η_l	Liquid viscosity.
ρ_l	Liquid density.
θ	Measured contact angle ($\theta \in [\theta_\mathrm{r};\ \theta_\mathrm{a}]$).
θ_a	Advancing contact angle.
θ_r	Receding contact angle.
θ_W	Wenzel contact angle.
θ_Y	Young contact angle.
$\theta_\mathrm{max}, \theta_\mathrm{min}$	Maximum and minimum contact angles (defined for the *tilted plate* method only).
Ca	Capillary number.

f	Force variation exerted on the suspending system (*Wilhelmy plate* method).
F	Relationship linking surface tensions to the contact angle formed at the three-phase line of contact.
g	Acceleration of gravity.
h	Liquid height in the capillary (*Washburn capillary rise* method).
H	Contact angle hysteresis (= θ_{a} - θ_{r}).
p	Total perimeter length of the solid substrate (*Wilhelmy plate* method).
ΔP	Pressure drop in the capillary (*Washburn capillary rise* method).
r_{eff}	Effective radius (ideal cylindrical pore radius, *Washburn capillary rise* method).
r_{drop}	Contact radius of an axisymetric liquid drop deposited on a flat solid substrate.
S_{ba}	Initial spreading coefficient of a liquid b over a surface a.
t	Time of the experiment.
V	Total immersed volume of solid substrate (*Wilhelmy plate* method).

ACKNOWLEDGMENTS

We would like to thank Brendan A. Patience for his contribution to the bibliographic map on contact angles. The professors Marie-Claude Heuzey and Pierre J. Carreau from Polytechnique Montreal (Montreal, QC, Canada) are gratefully acknowledged for their supervision and for their financial contribution to the scholarships of Charles Bruel and Salomé Queffeulou. We are thankful to the Fond de Recherche du Québec - Nature et Technologies (FRQNT) for kindly providing Charles Bruel with a scholarship (number 208324), and to the Faculté des Sciences University of Sherbrooke (Sherbrooke, QC, Canada) for his contribution to that of Salomé Queffeulou.

REFERENCES

[1] V. M. Starov, M. G. Velarde, C. J. Radke, A. Hubbard, Wetting and Spreading Dynamics, CRC Press, Boca Raton, FL, U. S. A. **2007**.

[2] C. Tropea, A. L. Yarin, J. F. Foss, Springer Handbook of Experimental Fluid Mechanics, Springer Berlin Heidelberg, Heidelberg, Germany **2007**.

[3] T. Young, *Philos. Transactions Royal Soc. Lond.* **1805**, *95*, 65.

[4] R. G. Good, *J. Adhesion Sci. Technol.* **1992**, *6*, 1269.

[5] M. Strobel, C. S. Lyons, *Plasma Process. Polym.* **2011**, *8*, 8.

[6] K. Mittal, Contact Angle, Wettability, and Adhesion, volume 6, CRC Press, London, United Kingdom **2009**.

[7] E. B. Troughton, C. D. Bain, G. M. Whitesides, R. G. Nuzzo, D. L. Allara, M. D. Porter, *Langmuir* **1988**, *4*, 365.

[8] C. D. Bain, G. M. Whitesides, *Sci.* **1988**, *240*, 62.

[9] W. A. Zisman, *J. Paint. Technol.* **1972**, *44*, 42.

[10] Y. Yuan, T. R. Lee, Contact angle and wetting properties, volume 51 of *Surface Science Techniques, Springer Series in Surface Sciences*, Springer, Berlin, Germany **2013**, pp. 3–34.

[11] M. Morra, E. Occhiello, F.Garbassi, *Adv. Colloid Interface Sci.* **1990**, *32*, 79.

[12] A. I. Bailey, *Proceeding 3rd Int. Conf. on Surf. Activity* **1960**.

[13] G. R. Lester, S.C.I. Monograph No. 25. Society of Chemical Industry, London, United Kingdom **1967**, pp. 57–98.

[14] A. Amirfazli, A. W. Neumann, *Adv. Colloid Interface Sci.* **2004**, *110*, 121.

[15] E. Bormashenko, *Adv. Colloid Interface Sci.* **2015**, *222*, 92.

[16] L. Boruvka, A. W. Neumann, *The J. Chem. Phys.* **1977**, *66*, 5464.

[17] W. D. Harkins, A. Feldman, *The J. Am. Chem. Soc.* **1922**, *44*, 2665.

[18] W. D. Harkins, *The J. Chem. Phys.* **1941**, *9*, 552.

[19] D. Bonn, J. Eggers, J. Indekeu, J. Meunier, E. Rolley, *Rev. Mod. Phys.* **2009**, *81*, 739.

[20] S. Torza, S. G. Mason, *Sci.* **1969**, *163*, 813.

[21] J. Reignier, B. D. Favis, M. C. Heuzey, *Polym.* **2003**, *44*, 49.

[22] J. Reignier, B. D. Favis, *Macromol.* **2000**, *33*, 6998.

[23] A. Marmur, *Soft Matter* **2006**, *2*, 12.

[24] C. O. Timmons, W. A. Zisman, *J. Colloid Interface Sci.* **1966**, *22*, 165.

[25] H. B. Eral, D. J. C. M. t Mannetje, J. M. Oh, *Colloid Polym. Sci.* **2013**, *291*, 247.

[26] A. Alghunaim, S. Kirdponpattara, B. Z. Newby, *Powder Technol.* **2016**, *287*, 201.

[27] M. Strobel, V. Jones, C. S. Lyons, M. Ulsh, M. J. Kushner, R. Dorai, M. C. Branch, *Plasmas Polym.* **2003**, *8*, 61.

[28] A. Terriza, R. Alvarez, F. Yubero, A. Borras, A. R. Gonzalez-Elipe, *Plasma Process. Polym.* **2011**, *8*, 998.

[29] S. Kirdponpattara, M. Phisalaphong, B. Z. Newby, *J. Colloid Interface Sci.* **2013**, *397*, 169.

[30] R. Woodward, Contact Angle Measurements Using the Drop Shape Method **2018**.
URL `http://firsttenangstroms.com/pdfdocs/CAPaper.pdf`

[31] A. Kietzig, *Plasma Process. Polym.* **2011**, *8*, 1003.

[32] M. Muller, C. Oehr, *Plasma Process. Polym.* **2011**, *8*, 19.

[33] B. Krasovitski, A. Marmur, *Langmuir* **2005**, *21*, 3881.

[34] E. Pierce, F. J. Carmona, A. Amirfazli, *Colloids Surfaces A: Physicochem. Eng. Aspects* **2008**, *323*, 73.

[35] L. A. Wilhelmy, *Annals Phys.* **1863**, *119*, 177.

[36] L. L. Popovich, D. L. Feke, I. Manas-Zloczower, *Powder Technoly* **1999**, *104*, 68.

[37] E. Chibowski, A. Ontiveros-Ortega, R. Perea-Carpio, *J. Adhesion Sci. Technol.* **2002**, *16*, 1367.

[38] S. Varennes, H. P. Schreiber, *The J. Adhesion* **2001**, *76*, 293.

[39] J. Drelich, J. S. Laskowski, M. Pawlik, S. Veeramasuneni, *J. Adhesion Sci. Technol.* **1997**, *11*, 1399.

[40] R. G. Good, N. R. Srivatsa, M. Islam, H. T. L. Huang, C. J. V. Oss, *J. Adhesion Sci. Technol.* **1990**, *4*, 607.

[41] D. Y. Kwok, A. W. Neumann, *Adv. Colloid Interface Sci.* **1999**, *81*, 167.

[42] R. N. Wenzel, *Ind. & Eng. Chem. Res.* **1936**, *28*, 988.

[43] A. B. D. Cassie, S. Baxter, *Transactions Faraday Soc.* **1944**, *40*, 546.

[44] G. Kumar, K. N. Prabhu, *Adv. Colloid Interface Sci.* **2007**, *133*, 61.

[45] G. Wolansky, A. Marmur, *Colloids Surfaces A: Physicochem. Eng. Aspects* **1999**, *156*, 381.

[46] C. D. Volpe, D. Maniglio, M. Morra, S. Siboni, *Colloids Surfaces A: Physicochem. Eng. Aspects* **2002**, *206*, 47.

[47] A. W. Neumann, R. J. Good, *J. Colloid Interface Sci.* **1972**, *38*, 341.

[48] C. Fang, J. Drelich, *Langmuir* **2004**, *20*, 6679.

[49] A. Y. Fadeev, T. J. McCarthy, *Langmuir* **1999**, *15*, 3759.

[50] S. Veeramasuneni, J. Drelich, J. D. Miller, G. Yamauchi, *Prog. Org. Coatings* **1997**, *31*, 265.

[51] C. Wang, S. Nair, K. J. Wynne, *Polym.* **2017**, *116*, 565.

[52] K. Grundke, T. Bogumil, T. Gietzelt, H.-J. Jacobasch, D. Y. Kwok, A. W. Neumann, *Prog. Colloid Polym. Sci.* **1996**, *101*, 58.

[53] J. T. Korhonen, T. Huhtamaki, O. Ikkala, R. H. A. Ras, *Langmuir* **2013**, *29*, 3858.

[54] V. Jones, M. Strobel, M. J. Prokosch, *Plasma Process. Polym.* **2005**, *2*, 547.

[55] R. D. Mundo, F. Palumbo, *Plasma Process. Polym.* **2011**, *8*, 14.

[56] J. M. Uilk, A. E. Mera, R. B. F. K. J. Wynne, *Macromol.* **2003**, *36*, 3689.

[57] A. Marmur, *Langmuir* **2003**, *19*, 8343.

[58] Y. Y. Yan, N. Gao, W.Barthlott, *Adv. Colloid Interface Sci.* **2011**, *169*, 80.

[59] J. D. Smith, R. Dhiman, S. Anand, E. Reza-Garduno, R. E. Cohen, G. H. McKinley, K. K. Varanasi, *Soft Matter* **2013**, *9*, 1772.

[60] Z. Lian, J. Xu, Z. Wang, Z. Yu, Z. Weng, H. Yu, *Langmuir* **2018**, *34*, 2981.

[61] J. Bico, U. Thiele, D. Quéré, *Colloids Surfaces A: Physicochem. Eng. Aspects* **2002**, *206*, 41.

[62] C. Ishino, K. Okumura, D. Quéré, *Europhys. Lett. (EPL)* **2004**, *68*, 419.

[63] C. Ishino, K. Okumura, *The Eur. Phys. J. E* **2008**, *25*, 415.

[64] M. Miwa, A. Nakajima, A. Fujishima, K. Hashimoto, T. Watanabe, *Langmuir* **2000**, *16*, 5754.

[65] C. J. van Oss, R. J. Good, R. J. Busscher, *J. Dispers. Sci. Technol.* **1990**, *11*, 75.

[66] W. A. Zisman, Relation of the Equilibrium Contact Angle to Liquid and Solid Constitution, volume 43 of *Advances in Chemistry*, chapter 1, **1964**, pp. 1–51.

[67] D. H. Kaelble, *The J. Adhesion* **1970**, *2*, 66.

[68] A. J. Meuler, J. D. Smith, K. K. Varanasi, J. M. Mabry, G. H. McKinley, R. E. Cohen, *ACS Appl. Mater. Interfaces* **2010**, *2*, 3100.

[69] V. B. Menon, D. T. Wasan, *Accounts chemical research* **1988**, *23*, 2131.

[70] E. Tsabet, L. Fradette, *Chem. Eng. Res. Des.* **2015**, *97*, 9.

[71] J. H. Zhang, S. Ravati, N. Virgilio, B. D. Favis, *Macromol.* **2007**, *40*, 8817.

[72] N. Virgilio, B. D. Favis, M. F. Pepin, P. Desjardins, G. L'Esperance, *Macromol.* **2005**, *38*, 2368.

[73] C. V. Thompson, *Annu. Rev. Mater. Res.* **2012**, *42*, 399.

[74] D. J. Srolovitz, M. G. Goldiner, *The J. The Miner. Met. & Mater. Soc.* **1995**, *47*, 31.

[75] T. Ryll, H. Galinski, L. Schlagenhauf, P. Elser, J. L. M. Rupp, A. Bieberle-Hutter, L. J. Gauckler, *Adv. Funct. Mater.* **2011**, *21*, 565.

[76] C. Bruel, R. Laraque, S. Omanovic, S. Coulombe, G. S. Patience, *Thin Solid Films* **2016**, *626*, 17.

[77] S. R. Challa, A. T. Delariva, T. W. Hansen, S. Helveg, J. Sehested, P. L. Hansen, F. Garzon, A. K. Datye, *J. Am. Chem. Soc.* **2011**, *133*, 20672.

[78] T. W. Hansen, A. T. DeLaRiva, S. R. Challa, A. K. Datye, *Accounts chemical research* **2013**, *46*, 1720.

[79] Clarivate Analytics, Web of Science^{TM} Core Collection **2017**, accessed on 7 February 2018.
URL `http://apps.webofknowledge.com`

[80] A. Perianes-Rodriguez, L. Waltman, N. J. van Eck, *J. Informetrics* **2016**, *10*, 1178.

[81] N. J. van Eck, L. Waltman, *Sci.* **2010**, *84*, 523.

[82] F. Bashtani, S. Kryuchkov, J. Bryan, B. Maini, A. Kantzas, *Can. J. Chem. Eng.* **2016**, *94*, 2091.

[83] M. Javidi, A. N. Hrymak, *Can. J. Chem. Eng.* **2016**, *94*, 2145.

[84] S. Maaref, M.-R. Rokhforouz, S. Ayatollahi, *Can. J. Chem. Eng.* **2017**, *95*, 1213.

[85] M. Zhang, Z. Du, F. Zeng, S. Y. Hong, S. Xu, *Can. J. Chem. Eng.* **2016**, *94*, 1402.

[86] H. Liu, L. ming Pan, J. Wen, *Can. J. Chem. Eng.* **2016**, *94*, 192.

[87] H. Azami, M. R. Omidkhah, *Can. J. Chem. Eng.* **2017**, *95*, 307.

[88] S. Fang, Y. Zhu, B. Chen, Y. Xiong, M. Duan, *Can. J. Chem. Eng.* **2016**, *94*, 2298.

[89] M. K. McGurn, E. N. Baydak, D. M. Sztukowski, H. W. Yarranton, *Can. J. Chem. Eng.* **2017**, *95*, 1909.

[90] K. M. T. Ahmmed, J. Montagut, A.-M. Kietzig, *Can. J. Chem. Eng.* **2017**, *95*, 1934.

[91] W. Xia, C. Niu, Y. Li, *Can. J. Chem. Eng.* **2017**, *95*, 475.

[92] T. Javanbakht, W. Raphael, J. R. Tavares, *Can. J. Chem. Eng.* **2016**, *94*, 1135.

[93] S. A. Kedzior, L. Graham, C. Moorlag, B. M. Dooley, E. D. Cranston, *Can. J. Chem. Eng.* **2016**, *94*, 811.

[94] M. Sedaghat, O. Mohammadzadeh, S. Kord, I. Chatzis, *Can. J. Chem. Eng.* **2016**, *94*, 779.

[95] A. Basit, K. KuShaari, P. Siwayanan, B. Azeem, *Can. J. Chem. Eng.* **2018**, *96*, 352.

[96] S. Vafaei, *Can. J. Chem. Eng.* **2016**, *94*, 315.

[97] T. Chen, F. Lin, B. Primkulov, L. He, Z. Xu, *Can. J. Chem. Eng.* **2017**, *95*, 281.

[98] B. Moradi, P. Pourafshary, F. Jalali, M. Mohammadi, *Can. J. Chem. Eng.* **2017**, *95*, 479.